EFFECT OF HEAT TREATMENT TO THE MORPHOLOGY OF TiO2 POWDERS VIA HYDROLYSIS ROUTE

This report is submitted in accordance with requirement of the University Teknikal Malaysia Melaka (UTeM) for Bachelor Degree of Manufacturing Engineering (Hons.)

by

MUHAMMAD FARIS AMIR BIN SUHAIMI

FACULTY OF MANUFACTURING
ENGINEERING 2021

DECLARATION

I hereby, declared this report entitled “Effect Of Heat Treatment To The Morphology Of TiO2 Powders Via Hydrolysis Route” is the result of my own research except as cited in references.

Signature : .....

Author’s Name : MUHAMMAD FARIS AMIR BIN SUHAIMI

Date : 2 SEPTEMBER 2021

APPROVAL

This report is submitted to the Faculty of Manufacturing Engineering of Universiti Teknikal Malaysia Melaka as a partial fulfilment of the requirement for Degree of Manufacturing Engineering (Hons). The member of the supervisory committee is as follow:

.....

(Madam Siti Rahmah binti Shamsuri)

SITI RAHMAH SHAMSURI
PENSYARAH
FAKULTI KEJURUTERAAN PEMBUATAN
UNIVERSITI TEKNIKAL MALAYSIA MELAKA
HANG TUAH JAYA, 76100 DURIAN TUNGGAL

ABSTRAK

Titanium dioksida (TiO2) adalah yang terdepan dalam penyelidikan luas mengenai penghasilan fotokatalis berkesan. Di antara banyak pemohon untuk aplikasi pemangkin foto, TiO2 adalah satu-satunya bahan yang sesuai untuk kegunaan industri pelapis kerana keseimbangannya yang kuat antara daya aktif yang efisien, kestabilan tinggi dan kos rendah. TiO2 mengalami transformasi fasa dari struktur anatase ke struktur rutil pada suhu yang lebih tinggi. Selain itu, struktur rutil adalah mustahak untuk dielakkan kerana struktur rutil tidak stabil seperti struktur anatase. Dalam penyelidikan ini, serbuk titanium dioksida (TiO2) akan dihasilkan dari bahan mentah titanyl sulfat (TiOSO4) melalui laluan hidrolisis. Nisbah antara TiOSO4 dan air suling adalah 1: 9 dan sintesis dilakukan pada waktu 8 jam. Serbuk TiO2 menjalani rawatan haba pada 3 suhu berbeza iaitu 200 ° C, 300 ° C dan 400 ° C selama 1 jam. Sampel yang diperlakukan dengan haba dan yang tidak diperlakukan panas selanjutnya dicirikan menggunakan XRD. Tujuannya adalah untuk menilai kesan rawatan haba pada suhu yang berbeza terhadap morfologi dan sifat fizikal serbuk TiO2. Hasil XRD menunjukkan bahawa ukuran kristalit diukur pada puncak tertinggi. Ini juga menunjukkan bahawa TiO2 tetap merupakan fasa anatase pada semua suhu yang dikaji.

ABSTRACT

Titanium dioxide (TiO2) is at the forefront of extensive research into the production of effective photocatalysts. Among the many applicants for photo-catalytic applications, TiO2 is almost the only substance suitable for the coating industrial use because of its strong balance between efficient photoactivity, high stability and low cost. TiO2 undergoes a phase transformation from anatase structure to rutile structure at higher temperature. Other than that, the rutile structure is a must to avoid because the rutile structure is not as stable as anatase structure. In this research, the titanium dioxide (TiO2) powder will be produced from titanyl sulphate (TiOSO4) raw materials via hydrolysis route. The ratio between the TiOSO4 and distilled water is 1:9 and the synthesizes is carry out at 8 hours' time. The TiO2 powder is undergoes heat treatment at 3 different temperatures which is 200°C, 300°C and 400°C for 1 hour. The heat treated and non-heat-treated sample is further characterized using XRD. The aim is to evaluate the effect of heat treatment at different temperatures to the morphology and physical properties of the TiO2 powders. The XRD results shows that the crystallite size measured at highest peak. It also shows that the TiO2 is remained anatase phase at all studied temperature.

DEDICATION

Only

My beloved father, Suhaimi bin Yunus

My appreciated mother, Zanariah binti Abd Razak

My adored sisters and brother,

For giving me moral support, money, cooperation,

Encouragement and understandings

Thank You So Much

ACKNOWLEDGEMENT

In the gracious of God, the most gracious, the most merciful, with the highest praise to God that I managed to complete this final year project successfully without difficulty.

My respected supervisor, Madam Siti Rahmah binti Shamsuri. Her support, direction, criticism and feedback had been a strong guidance for me throughout the completion of this project.

Also, I would like to extend my thanks to my friends for their comments and support. Besides, I would also like to thank all the staff and technicians on completion of my project for their support, indirect or direct feedback.

TABLE OF CONTENTS

LIST OF TABLES

LIST OF FIGURES

LIST OF ABBREVIATIONS

SEM	-	Scanning electron microscope
UV	-	Ultraviolet
XRD	-	X-ray diffraction
ART	-	Anatese rutile transformation
TEM	-	Transmission electron microscope
ISO	-	International organization for standard
TiO2	-	Titanium Dioxide
FTIR	-	Fourier-transform infrared spectroscopy
DTA	-	Differential thermal analysis
TiOSO4	-	Titanyl sulfate

CHAPTER 1

INTRODUCTION

1.1 Background of study

Due to its broad range of applications, especially in the field of photocatalysis, titanium dioxide (TiO2) is a resource of great importance, as it is widely recognised for its outstanding photocatalytic activity. A photocatalyst refers to a " catalyst that accelerates the solar photo reaction " and the following requirements need to be met in order to become a photocatalyst: the photocatalyst does not engage or be consumed directly in the reaction; and needs to include other mechanism routes from current photo reactions and accelerated reaction rate (Lee et al., 2013). TiO2 has been confirmed to be commonly used for the degradation of hazardous and toxic organic contaminants by photocatalysts. This material has been used on the exterior surfaces of buildings for self-cleaning applications. It also demonstrates excellent chemical stability, high refractive index, excellent ultraviolet absorption and photochemical behaviour, which are required to play important roles in pigments, catalysts and supports, ceramics, inorganic membrane, water purification, etc (Amin et al., 2011). As we note, there are three crystal structures of titanium dioxide (TiO2) which are anatase, rutile and brookite. The rutile phase has the highest refractive index and ultraviolet absorptivity among them, so it has wide applications in pigments, paints, ultraviolet absorbents. In the other side, the anatase step is chemically and optically active and is also ideal for catalysts and supporters. Both two structures of crystals have their own temperature levels of stability which can be regulated by heat treatment and often by dopants.

1.2 Problem Statement

TiO2 undergoes a phase transformation from anatase structure to rutile structure at higher temperature. It is commonly accepted that anatase is a more capable photocatalyst (compared to rutile and brookite), which is evident from the numerous studies that have highlighted the photocatalytic application of TiO2 (Jing et al., 2008).

This changes in crystal structure and crystallite size of TiO2 powders reduce the photocatalytic property of coating. It is expected that, the calcined TiO2 powders displayed greater crystallinity and thicker coating relative to the as-synthesized powder. The calcination temperature of not only facilitates the growth of grain and the crystallised size of the as-synthesized TiO2 powders, but also decreases the porosity of the agglomerated powder by the densification of the particles. Thus, it is vital to study the optimal temperature used to heat treated the TiO2 powder to obtain the desired TiO2 type.

1.3 Objective

a. To evaluate the crystallite size of TiO2 with different heat treatment temperature using XRD Analysis.

b. To review the effect of heat treatments at different temperatures on the morphology of the TiO2 powders.

1.4 Scope of study

In this project, hydrolysis will be use as the preparation method to synthesize the TiO2 powder. The reason for using this method is because it is a low-cost process, and it is also a low temperature process which is can avoid from the TiO2 engaging a phase transformation from anatase to rutile. Other than that, hydrolysis is a simple method and can easily be handled without any extra precautionary steps. In order to examine the effects of the heat treatment on morphology and physical properties, 3 different temperatures is : 200°C, 300°C and 400°C for 1 hour. SEM, XRD and FTIR have employed for characterization of the heat treated TiO2 powders.

1.5 Thesis Organization

This thesis consists of five chapters. Chapter 1 is the introduction of this thesis. In this chapter it consists of background of study, problem statement, objective, and scope of study of this project. In Chapter 2, a literature review of previous study on the photocatalytic materials, the details of TiO2 material and the development and properties of TiO2 such as when does it become anatase or rutile. Other than that, in this chapter it will review the different methods for synthesized TiO2 such as hydrolysis, hydrothermal, and others based on past research that have been carried out before. The development of TiO2 material and heat treatment for TiO2 powder will included in this chapter. Chapter 3 will describe the details methodology that will be carry out in this project. This includes the flow chart of the step in the project and the details explanation about each process as well as the method that will be used to characterize the heat treated TiO2 powders. Chapter 4 is about the result and discussion of this project. In this chapter we will discuss about the data and interpret it on what all this project about. Last part of the thesis organization Chapter 5, conclusion. A conclusion is an essential element of the paper since it offers closure for the reader while also reminding the reader of the paper's contents and significance. It achieves this by taking a step back from the details to look at the broad picture of the paper. In other words, it serves to remind the reader of the primary point.

CHAPTER 2

LITERATURE REVIEW

This section would quickly clarify all the relevant topics of this research project. This segment focuses on TiO2 materials, the TiO2 synthesised process and the development of TiO2.

2.1 Photocatalytic Material

Pawar et al., (2018), stated as a photocatalyst, titanium dioxide (TiO_2) has attracted substantial attention for a long time and is considered as one of the most promising materials for commercial use due to its outstanding optical and electronic properties, photoactivity, high chemical stability, low cost, nontoxicity, reusability, and eco-friendliness. Much more attention has been focused on the different preparation methods of TiO_2 in order to improve its performance compared to commercial TiO_2 powders (for example, Degussa P25).

A photocatalyst is a medium that consumes light to raise its energy level and gives the reacting substance such energy to produce a chemical reaction. If the photocatalyst absorbs the light, the valence electron band induces positive hole reactions with electrons. Those positive TiO2 holes lead to OH radicals, which are decomposing radioactive compounds by water or dissolved oxygen. The radical OH is stronger to sterilize or disinfect than chlorine or ozone.

The primary prerequisite of an effective photocatalyst semiconductor is that the redox ability of the charge pair, i.e. e-/h+, is part of the photocatalyst band gap domain. The energy level in the lower band of the conduction decides the photoelectrons' reduction, while the energy level in the highest band of the valence decide the photogenerated holes' oxidizing potential (Gupta et al., 2010).

Gupta et al., (2010) stated that TiO2 is a photocatalyst ideal and the reference point for the efficiency of photocatalysis. TiO2 is inexpensive, non-toxic and photostable. Its hole is intensely oxidising and selective redox. For these purposes, at the interface of TiO2 illuminated photocatalysts, several novels, heterogeneous photocatalyst reactions have been documented and TiO2 bases for environmental cleanup applications have been extensively researched. The main downside is that visible light is not reflected. Several methods have been extensively studied to solve this challenge, including dye sensitization, doping, combination and capping TiO2

2.2 TiO2 materials

In the last five decades a substantial amount of TiO2 study has been conducted and numerous review papers have been written on different aspects of TiO2 to explain and summarize the progress made in this field. In this analysis, the properties of TiO2, which make it ideal for photocatalyst functions, and the different methods used to enhance its efficacies, including dye sensitization, doping, capping are addressed. Applications for environment and electricity, including photocatalytic treatment of wastewater, degradation of pesticides and the division of water into the generation of hydrogen by TiO2 are summarized.

Based on review paper by Gupta et al. (2010),. There are four widely recognized TiO2 polymorphs: anatase (tetragonal), brookite (orthorhombic), rutile (tetragonic) and TiO2(B) (monoclinic) in nature. In addition to these polymorphs, the rutile phase was synthesized with two more high-pressure variants. The system consists of TiO2 (ii), PbO2, and the hollandite structure of TiO2 (H). Only crystal (Table 2.1) and rutile, anatase and brookite polymorphs characteristics are included in this study.

Table 2.1: Crystal structure data for TiO2

Properties	Rutile	Anatase	Brookite
Crystal structure	Tetragonal	Tetragonal	Orthorhombic
Lattice constant (Å)	$a = 4.5936$ $c = 2.9587$	$a = 3.784$ $c = 9.515$	$a = 9.184$ $b = 5.447$ $c = 5.154$
Space group	$P4_2/mnm$	$I4_1/amd$	Pbca
Molecule (cell)	2	2	4
Volume/ molecule ($Å^3$)	31.2160	34.061	32.172
Density (g cm^{-3})	4.13	3.79	3.99
Ti–O bond length (Å)	1.949 (4) 1.980 (2)	1.937(4) 1.965(2)	1.87–2.04
O–Ti–O bond angle	81.2° 90.0°	77.7° 92.6°	77.0°–105°

The tetragonal structure of Rutile TiO2 comprises 6 atoms per unit cell (Figure 2.1). The octahedron TiO6 is somewhat skewed. The rutile phase is stable at maximum temperatures and pressures of 60 kbar, and TiO2 (II) is the thermodynamically advantageous phase. Zhang et al. find that after a certain particle size, anatase and brookite systems have turned into a rutile phase with a rutile phase more stable than a particle size anatase over a size of 14 nm. When the rutile phase was formed, it evolved much more rapidly than the anatase. The photocatalyst activity in the rutile process is normally very low. Sclafani et al. however concluded that depending on the conditions of preparation the rutile process could be active or inactive.

Tetragonal configuration is also present in anatase TiO2, but the TiO6 octahedron distortion is significantly greater during the anatase step, as seen in Figure 2.1. Muscat et al. found a stabilizer of the anatase phase than rutile at 0k, but the difference in energy between the two phases is slight (total 2 to 10kJ/mol). Due to its higher electron motility, low dielectric constant and lowered density, the anatase structure is favored over other polymorphs for solar cell applications. Due to a marginally higher Fermi level lower propensity to adsorb oxygen and higher hydroxylation levels in the anatase process, the increased photo reactivity is. The reactivity (001) of facets in the anatase crystal has been stated by Selloni et al. (2008)

to be more significant than (101). Yang et al. (2008) synthesized standardized anatase glass with 47% (001) face use as a morphology regulating agent hydrofluoric acid.

The orthorhombic crystal system is owned by Brookite TiO2. The cell unit is generated by the TiO6 octahedra edge-sharing and consists of 8 formula units of TiO2 (Figure 2.1). It is also more complex, has greater cellular volumes and is therefore the least dense of the three types.

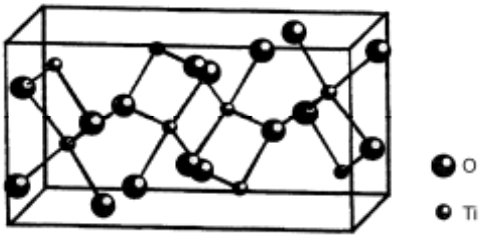

Figure 2.1: Lattice structure of TiO2.

2.3 Method of synthesized TiO2

Titanium dioxide (TiO2) nanoparticles are one kind of important and promising photocatalysts due to their special optical and electronic properties in photocatalysis. Various methods can be used in synthesising TiO2, including the sol-gel technique, chemical vapour deposition (CVD) and hydrothermal methods. Their properties, which are determined by the preparation method, are very crucial in photocatalysis.

2.3.1 Chemical Vapour Deposition (CVD)

Malekashi et al. (2013) stated that Vapor deposition means any technique in which material is condensed into a solid-phase substance in a vapour condition. These techniques are usually used to create coatings that change the mechanical, electrical, thermal, optical, resistant to corrosion and wear characteristics of different substrates. Thermal energy heats and promotes the deposition reaction in CVD procedures the gases in the coating Chamber. The process parameters in CVD include the flow rate, gas structure, deposition temperature, pressure and deposition chamber shape, where the deposition may be adjusted to have the required material nanoforms.

Djerdja et al. (2010) reported nanocrystalline TiO2films by CVD on different substrates at relatively low temperature of 320 ◦C using TiCl4 as a precursor and found that the nature of substrates influences the size and distribution of nanograins in the films. Byun et al. prepared TiO2 thin films at 287–362 ◦C using titanium (IV) tetraisopropoxide (TTIP) precursor and O2 gas.

Figure 2.2 displays the typical Tio2 film XRD pattern, obtained in the 10–100℃ diffraction-angle diameter of the TiO2 (formed on the glass substrate at 400 ◦C). The correspondence of the observed and the standard values support the phase pure TiO2 anatase and a tetragonal structure deposited film. By expanding the (101) diffraction peak at 25.35 ◦C with a famous Scherrer formula, crystallite sizes of 10 ± 2 nm were found.

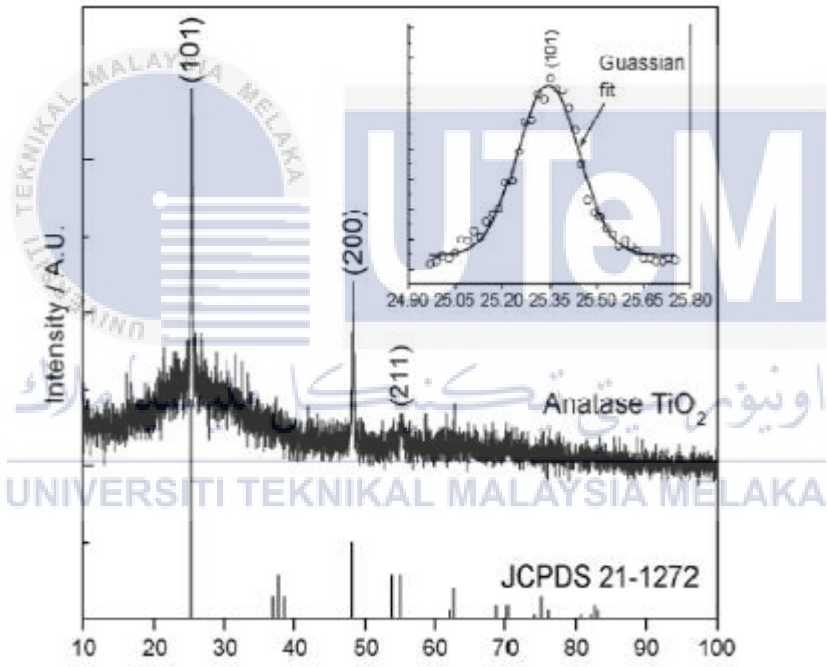

Figure 2.2: X-ray diffraction spectra of chemical vapor deposited anatase TiO2 thin film

2.3.2 Hydrohthermal

Maleksashi et al. (2013) state that, hydrothermal synthesis typically occurs with or without teflon liners at regulated temperature or pressure in aqueous solutions in the steel pressurised containers known as autoclaves. The temperature may be higher than the water boiler, exceeding the vapour saturation pressure. The inside pressure is primarily determined by the temperature and quantity of solution

introduced to the autoclave. It is a technique used frequently in the ceramics industry for the creation of tiny particles.

The hydrothermal treatment of peptitized precipitates of a titanium precursor with water can produce TiO2 nanoparticles. Appendix 0,5M titanium butoxide solution in deionized water ([H2O]/[Ti]) = 150) was used in precipitation, followed by tetraalkylammonium hydroxides peptizing at 70°C for 1 hour. The precipitates were subsequently prepared. In the Figure 2.3 you can see a typical TEM pictures of TiO2 hydrothermal nanoparticles.

Figure 2.3: TEM images of TiO2 nanoparticles prepared by the hydrothermal method.

TiO2 nanoparticles were produced utilising a hydrothermal technique in addition to TiO2 nanoparticles. TiO2 nanorods have been produced by Zhang et al. in the presence of acids or inorganic salts by treating the TiCl4 solution dilutable in 59.85-149.85 ºC for 12 hours. Figure 2.4 shows the typical TEM picture of the hydrothermally produced TiO2 nanorods. Figure 2.5 shows TiO2 nanowires' SEM pictures.

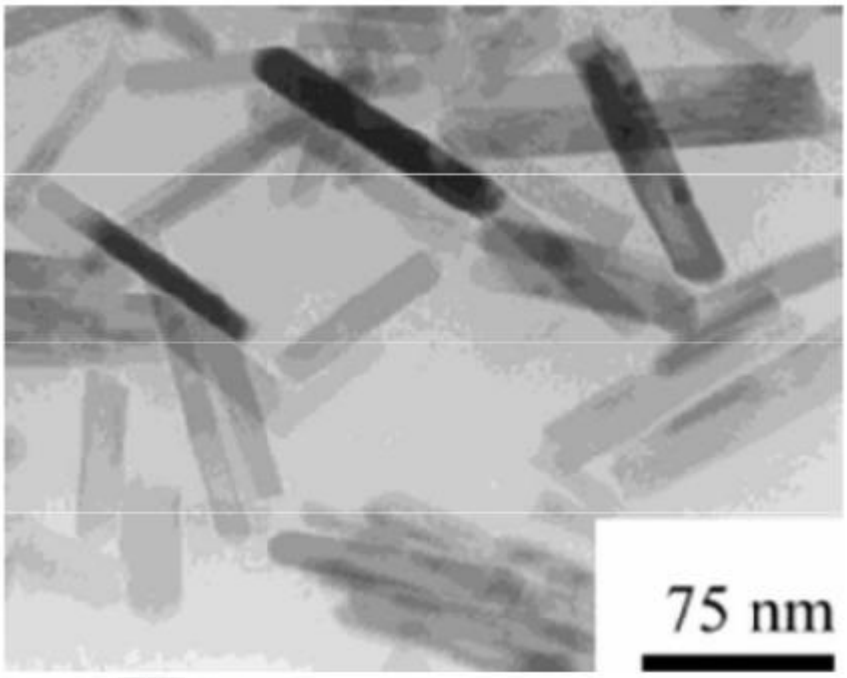

Figure 2.4: TEM image of TiO2 nanorods prepared with the hydrothermal method

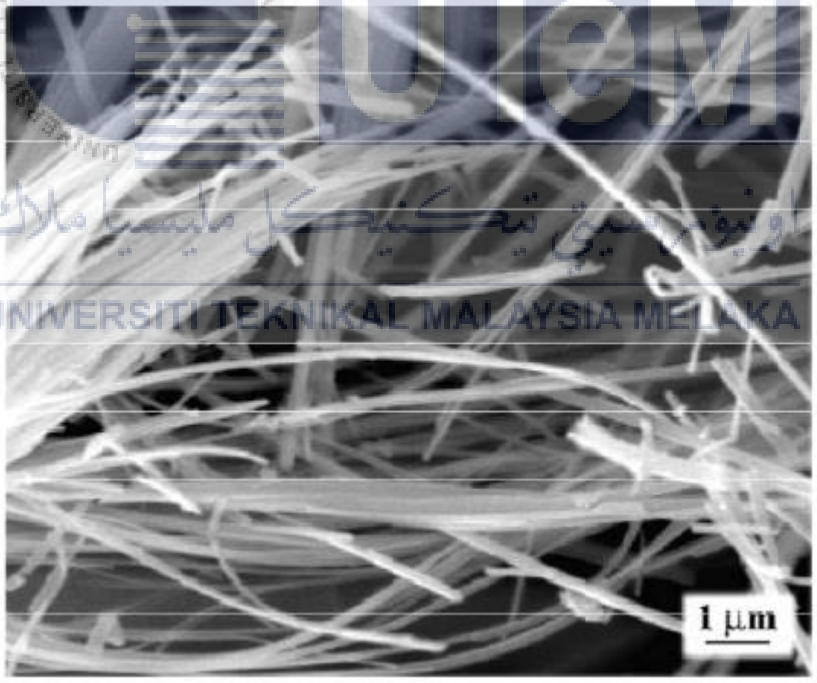

Figure 2.5: SEM images of TiO2 nanowires prepared with the hydrothermal method

The hydrothermal technique has also been used to manufacture TiO2 nanotubes. 2 g TiO2 white power has been put in a teflon-lined automoclave with a capacity of 100 ml during a typical preparation operation. The autoclave was then completed in a stainless tank with 80 mL aceous 10 M NaOH solution, kept at a temperature of 130 − C for 24

hours. The sample collected was filtered and distilled with water multiple times after it was cooled to room temperature. The products produced were then collected and washed for 24 hours with an aqueous HCl solution (pH 1.6) then washed many times with distilled water until the pH value became 7. The products were finally breathed into the air at 400 ◦C for 2 hours. Figure 2.6 illustrates the typical TEM picture of the hydrothermal TiO2 nanotubes produced.

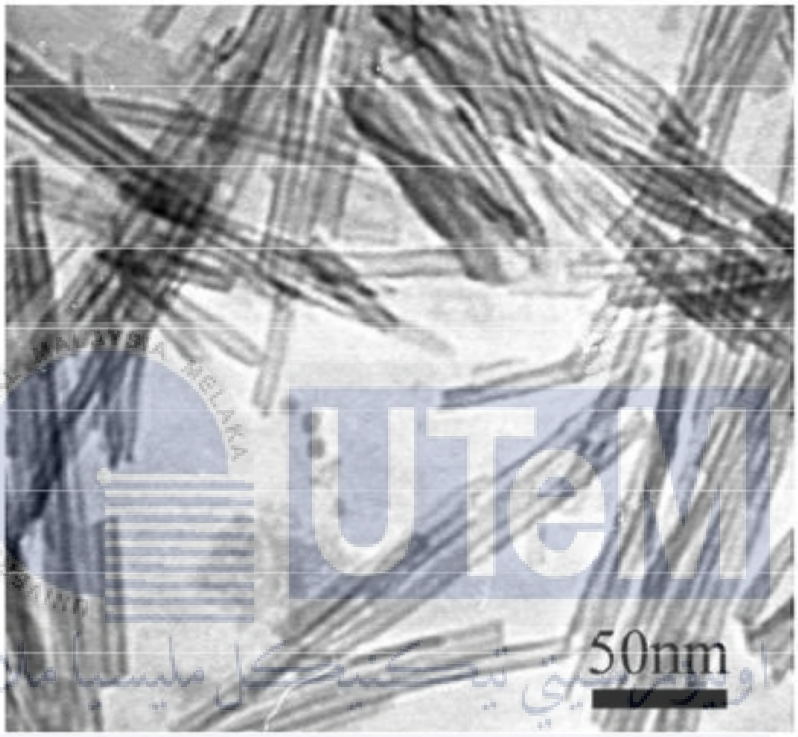

Figure 2.6: TEM images of TiO2 nanotubes prepared with the hydrothermal method.

2.3.3 Microwave

Amirudha et al. (2010) has synthesized TiO2 using microwave, they used two separate conditions. In the first sample, 2.94 mL of Ti(i OPr)4 was dissolved in 30 mL of dried ethanol and in the second batch, 5 mL of hydrazine hydrate was added to the Ti(i OPr)4 solution in ethanol, prepared in the same manner as in the first test. The oxide samples collected from these two batches are TiO2(E) and TiO2(HH) respectively. A solution of surfactant poly (vinyl pyrrolidone) (PVP, molecular weight) 360000 was applied to both solutions; 0.3 g of PVP was dissolved in 15 mL of ethanol and the consolidated (reactant) solution was stirred for 30 min. The reactive

solution, taken in a round-bottomed flask, was subjected to microwave irradiation at a capacity of 800 W in a domestic microwave oven (2.45 GHz) fitted with a reflux condenser mounted outside the oven.29 The length of the irradiation was 5 min, during which the resulting colloidal solution was centrifuged to extract the solid powder product which was heated in air at 500 °C for 1 h.

Powder X-ray diffraction patterns of TiO2(E) and TiO2(HH) oxides as seen in Figure 2.7. The patterns clearly indicate that both samples are well crystallised. The patterns could be indexed to the titanium of the anatase process. The lack of peaks at the Bragg angles of 27.5°, 39.3° and 54.2° confirms the absence of a rutile process in the samples.

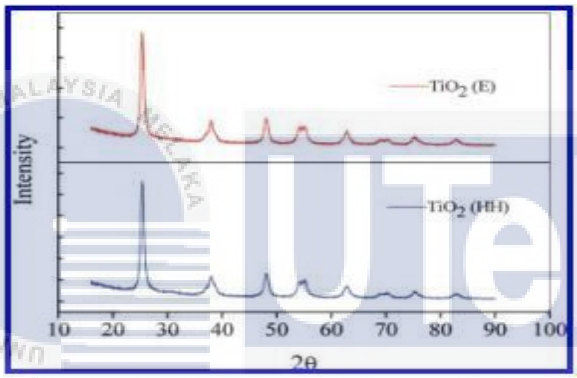

Figure 2.7: X-ray diffraction (XRD) patterns of TiO2(E) and TiO2(HH).

2.3.4 Hydrolysis

The hydrolysis method is essentially the simplest method of synthesising the TiO2 content. Unfortunately, several researchers did not use this technique to synthesise the TiO2, which be a project guide. Mahshid et al. (2007) in his research, the processing of TiO2 colloids in the nanometer range can be effectively carried out by hydrolysis and condensation of titanium alkoxides in aqueous media. In the presence of water, alkoxides are hydrolyzed and then polymerized to create a three-dimensional oxide network. These reactions can be schematically presented as follows:

$$Ti(OR)4 + 4H2O \rightarrow Ti(OH)4 + 4ROH \text{ (hydrolysis)}$$

$$Ti(OH)4 \rightarrow TiO2xH2O + (2 - x)H2O \text{ (condensation)}$$

where R is ethyl, i-propyl, n-butyl, etc.

Figure 2.4 shows the XRD pattern of the prepared powder in the different pH. When the pH level of the solution is higher than 2, a white suspension of rough precipitant is formed immediately after hydrolysis reaction. Otherwise, when the pH level of the solution is 2, a homogenous suspension of fine particles is formed. The crystallite size of the particles has been estimated from the Debye–Scherrer's equation using the XRD line broadening as follows: $B = k\lambda \, s \cos \theta$ (1) where s is the crystallite size, λ the wavelength of the X-ray radiation (Cu K = 0.15406 nm), k a constant taken as 0.94, θ the diffraction angle and B is the line width at half maximum height. The (1 0 1) plane diffraction peak is used for anatase and (1 1 0) peak for rutile.

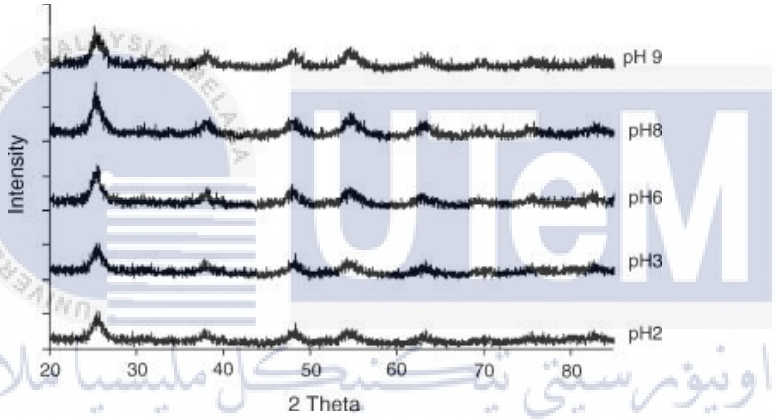

Figure 2.8: XRD patterns for TiO2 particles obtained from different pH solutions and dried at 100 ◦C for 3 h.

From this research, it is found that a greater particle size with spherical morphology is obtained at higher calcination temperatures. In the case of a sample calcined at 400 C (Figure 2.9), the particle size is almost 100 nm.

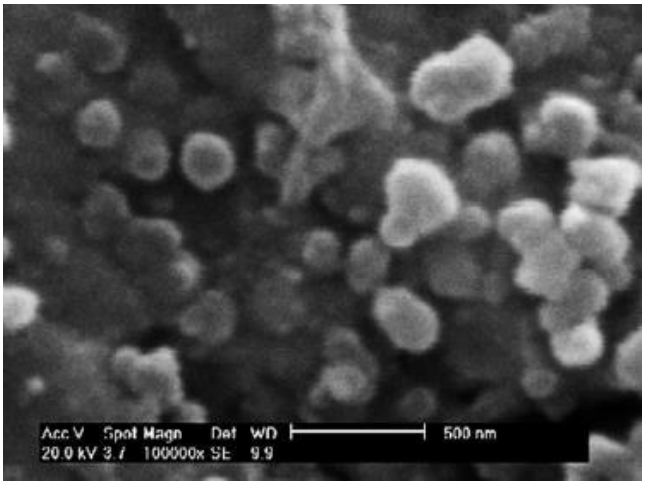

Figure 2.9: SEM micrographs of powders prepared at 400 ◦C

2.4 Development of TiO2

Throughout the decade of studies, there have been many developments in TiO2 as the TiO2 material is one of the most promising photocatalytic materials in the world.

2.4.1 Nanotubes

Naturally, TiO2 largely consists of the anatase, rutile and brookite in three crystalline phases. Moreover, a number of high-pressure polymorphs, such TiO2(B) may be hydrothermally synthesized, and several synthetic layered phases were described also.

Lee et al (2014) stated that for example, TiO2 structures synthesised at low temperatures are generally amorphous, such as those of anodic or sol−gel-based methods. Generally, the phase change is approximately 300–400°C and 500–700°C from anatase to rutile. The precise temperature of conversion depends on various parameters such as contaminants, texture of primary particle sizes and structural strain. The most common phases in practical applications are anatase and rutile. Nonetheless, most recent work appears to show that, in TiO2 nano tubing and

comparable geometries, unique TiO2 may be produced via Li (lithium) cycling of TiO2 nanotubes, previously considered to exist under high pressures only.

The rutile is believed to be a thermodynamically stable phase as a bulk system (extended lattice). Many test and theoretical studies suggest that anatase with crystallite sizes of less than around 10–30 nm is the most stable phase for nanoscale materials. Some study has shown that tube diameter-dependant phase stabilisation is shown in nanotube walls for anodic TiO2 nanotube layers, which are produced and rinsed on a titanium substrate, where rutile rather than anatase develops on rinsing amorphous tubes for small diameters (<30 nm).

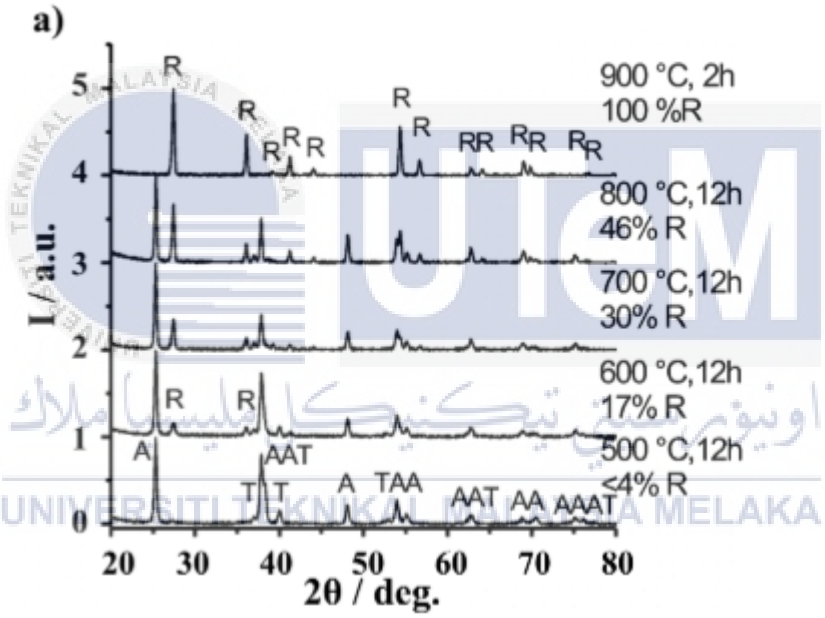

Figure 2.10: XRD spectra of nanotubes annealed at 500, 600, 700, 800, and 900°C for 12h.

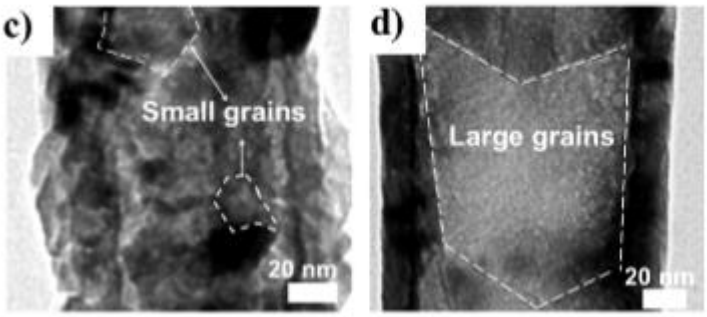

Figure 2.11: TEM images of annealed (c) double wall and (d) single wall TiO2 nanotubes.

2.4.2 Nanoparticles

Behnajady et al. (2011) carried out an exeperiment to produced nanoparticles calcinated at different temperatures for 3 h to examine the influence of calcination on the crystallite size, phase composition and photocatalytic activity of the TiO2 nanoparticles. Calcined samples of the XRD at 350°C, 450°C and 750°C at various temperatures (Fig. 2.12(a–c)) indicate an amorphous sample calcinated at 350° C. As in the XRD spectrum, the anatase phase percent reduces with the increasing temperature of calcination while the rutile phase grows, the anatase phase translates entirely into rutile phase at 750 °C. Increased calcination temperature will increase anatase and rutile phase crystallite size. The samples calcined at different temperatures were reported in Table 2.2 on crystallite size and the phase.

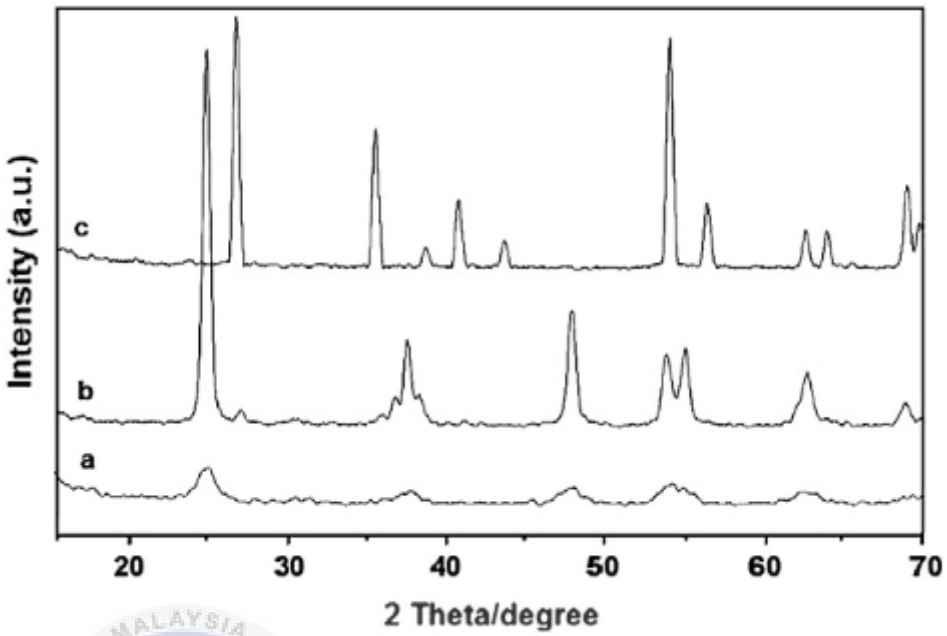

Figure 2.12: XRD patterns of TiO2nanoparticles calcined at different temperatures:(a) 350 °C, (b) 450 °C, (c) 750 °C.

Table 2.2: Phase content and crystallite size of TiO2nanoparticles calcined at different temperatures.

Calcination temperature (°C)	Amount of each phase %	Crystallite size (nm)
350	A: 100, R: –	D_A: 5, D_R: –
450	A: 95, R: 5	D_A: 15, D_R: 12
750	A: –, R: 100	D_A: –, D_R: 22

Results of Figure 2.13 show that TiO2 nanoparticles' photocatalytic activity declines from 350 ° to 750 °C, and their calcination temperature rises. This decrease in nanoparticles' activities may be rationalised because of the growth of crystallite nanoparticles, nanoparticle agglomeration, less absorbed H2O and the rutile stage increases. Particles also have a smaller diameter in low calcination temperature, the increase in photocatalytic activity may be explained by the quantum size effect at such temperatures. The quantum size of nanoparticles is within a range of 1-10 nm.

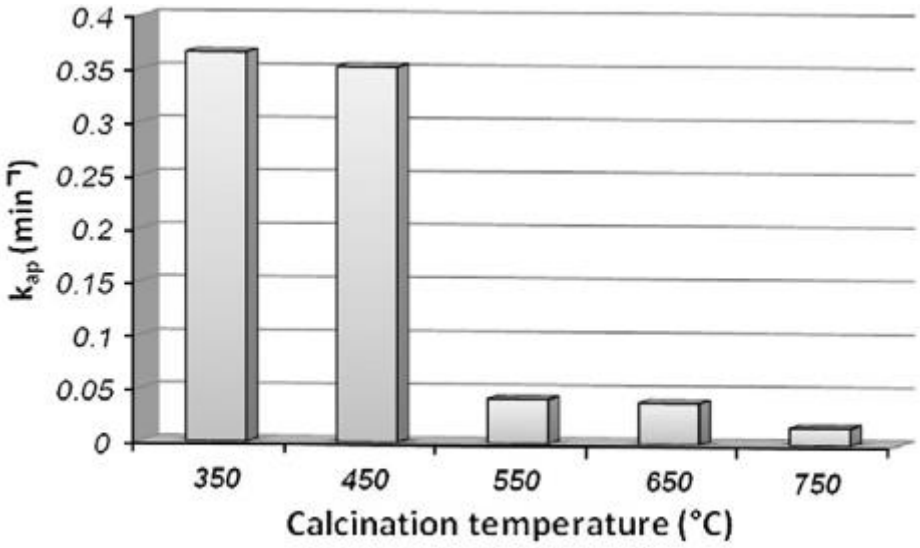

Figure 2.13: Effect of calcination temperature on photocatalytic activity of TiO2nanparticles

2.4.3 Porous TiO2

Zhou et al. (2018) stated that porous TiO2 is an ideal carrier for loading with elemental iron owing to its wide surface area and negative surface load. Porous TiO2 was synthesised as a silica monolith, which was hierarchically porous, and a block copolymer for mesoporous shapes was used as a prototype. In restricted areas, the crystalline TiO2 retained the porous framework and its strong crystallinity.

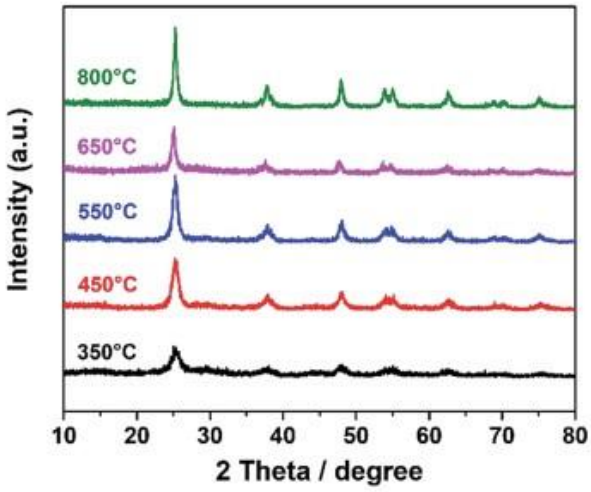

Figure 2.14: XRD pattern of DTT, which was calcined at different temperatures.

According to the XRD spectra shown in figure 2.14, all the TiO2 samples were in the anatase process. The amplitude of the diffraction peak improved, and the full width was decreased by half the limit (FWHM) with a rise in temperature. There was no noticeable shift in the XRD spectra when the temperature was greater than 450 C. These findings showed that the anatase structure of TiO2 can be preserved even at a calcination temperature of up to 850 C. Usually, TiO2 changes to the rutile process at such a high temperature. Preservation of the anatase process indicated that the transformation step was constrained in compressed porous space during calcination. This restriction was possibly related to the nuclear rearrangement, which contributed to a shift in the volume of the sample, as the operation was quite restricted in small spaces. Such containment culminated in difficulties in the incidence of the transition process.

Sun et al. (2017) state that in determining the porosity and homogeneity of the TiO2 mesoporous layer, the size and mass fraction of (polystyrene) PS spheres are critical Scan electron microscopic was used to investigate the surface morphology of the TiO2 films.

As shown in figure 2.15, holes are seen in the film mp-TiO2 created by the paste paste with PS spheres (PS-0), unlike the TiO2 layer, which spins the paste without the paste PS spheres (PS-0). A few holes with an average dimension of 70nm are generated on the surface of Mp-TiO2 layers for a low percentage of 0.5% of the PS spheres in the paste (PS-0.5). In case of a growth in the mass fraction of the PS spheres in TiO2 paste, a lot of holes with an average size of 80nm are produced, which are PS-1.0. The pore diameters are virtually same on average for PS-0.5 and PS-1.0 and the distribution of the poles is consistent. As the mass fraction of PS spheres rises to 1,5 wt% (PS-1,5), the high volume fraction of PS spheres and the conglomerate of PS spheres into the TIO2 paste produced holes of relative bigger apertures (94nm).

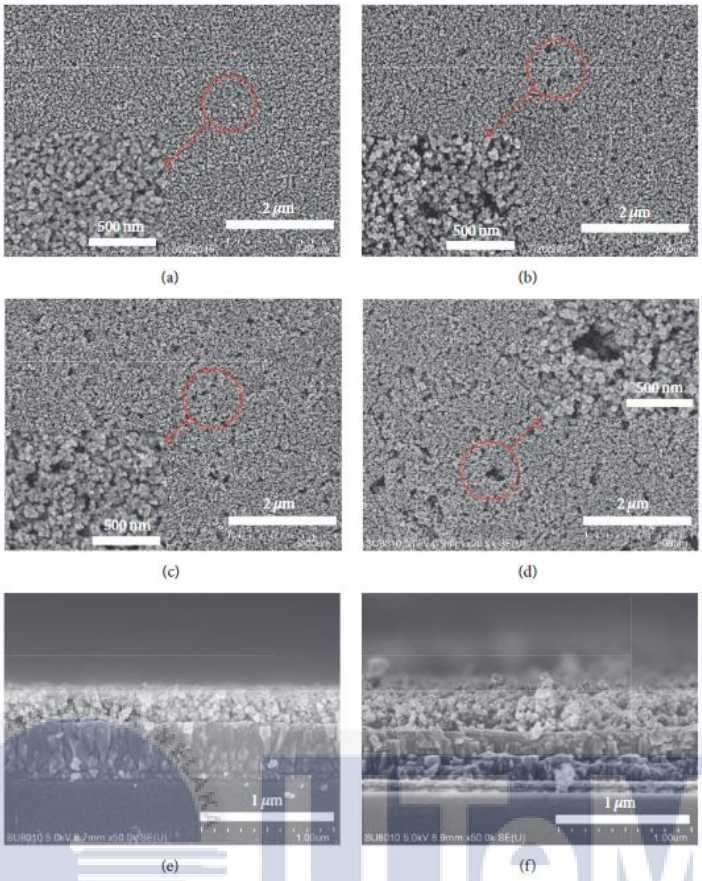

Figure 2.15: Plane-view SEM images of (a) PS-0, (b) PS-0.5, (c) PS-1.0, and (d) PS-1.5. Cross-sectional SEM images under high magnificationof (e) PS-0 and (f) PS-1.0.

In comparison with the PS-1.0, the pores distribution is inhomogeneous. In cross-sectionally SEM sample pictures PS-0and PS-1.0 (Figures 2.15(e) and 2.15(f) the pore structure could be detected clearly. The samples PS-0 and PS-1.0 are 260nm and 360nm as shown in Figures 2.15(e) and 2.15(f). In addition, the sample PS-1.0 porous structure is looser than the PS-0 sample. There are tightly packaged TiO2 nanoparticles and practically no holes in the PS-0 sample of the nanoparticles. The cross-sectional SEM picture in PS-1.0 (Figure 2.15(f)) may nonetheless be recognised as pores. Not just on the mp-TiO2-foil surface but throughout the film the pores appeared. Due to the existence of larger pores in the film, sample PS-1.0 is thicker than sample PS-0.

2.5 Heat Treatment of TiO2 powders

Toibah et al. (2016) carry out a heat treatment of the TiO2 powders. Figure 2.16 shows the DTA curve of the as-synthesized TiO2 powders. The DTA curve of assynthesized TiO2 powders indicates that a broad endothermic peak exists at ca. 75°C which attributes to desorption of water molecules. The partial presence of water molecules on the surface of the precursor was expected as the reaction was carried out using distilled water as the aqueous media. There is a small endothermic peak maximum at ca. 180°C due to loss of organic residues and chemisorbed water. An exothermic peak observed at 480°C can be attributed to the progressive growth of crystallites size and crystallinity of the TiO2 powders. The exothermic peak with a maximum at ca. 950°C is corresponded to the phase transformations from anatase phase to rutile phase.

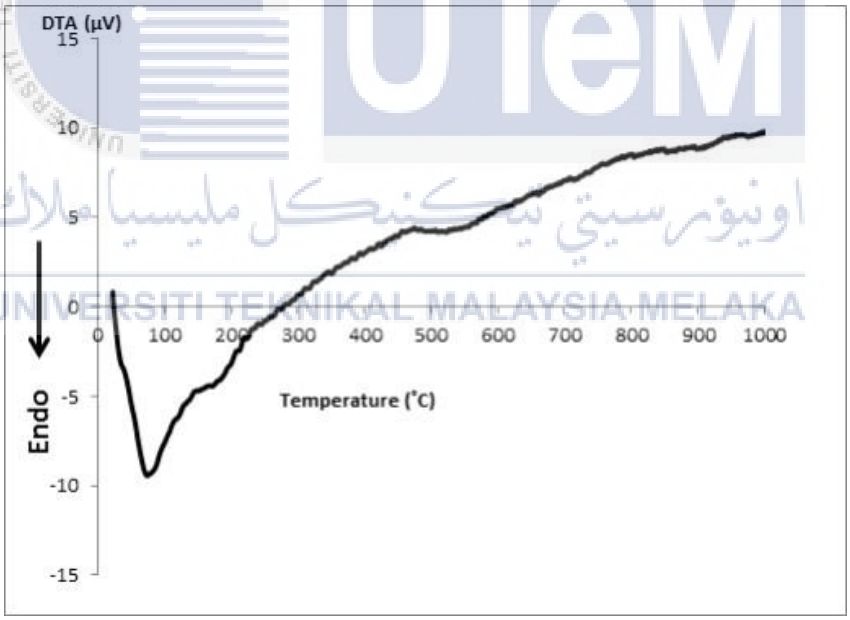

Figure 2.16: DTA curve recorded in air with a 10°C/min heating rate for as-synthesized TiO2 powder.

An experiment on heat treatment by Salim et al. (2011) stated that Figure 2.17 shows the powder morphologies formed by the FE-SEM. The synthesised TiO2 powders have an agglomerated composition composed of very fine nano-primary (1°) particles. Nanoparticles are agglomerated to create a secondary (2°) particle with a

scale of approximately 2 μm. These 2° particles are further agglomerated into tertiary (3°) particles of a scale of 17 μm as seen in Figure 2.17a–c. The FE-SEM picture also shows that post-treatment would not change the shape and scale of the 2° and 3° particles. On the opposite, the higher magnification images in Figure 2.17d–f indicate the development of 1° particle structure into more well-defined crystals after post-treatment, supporting the rise in 1° particle size due to post-treatment. Higher magnification photos often show greater annealed TiO2 particle sizes (Figure 2.17e) than hydrothermal TiO2 (Figure 2.17f).

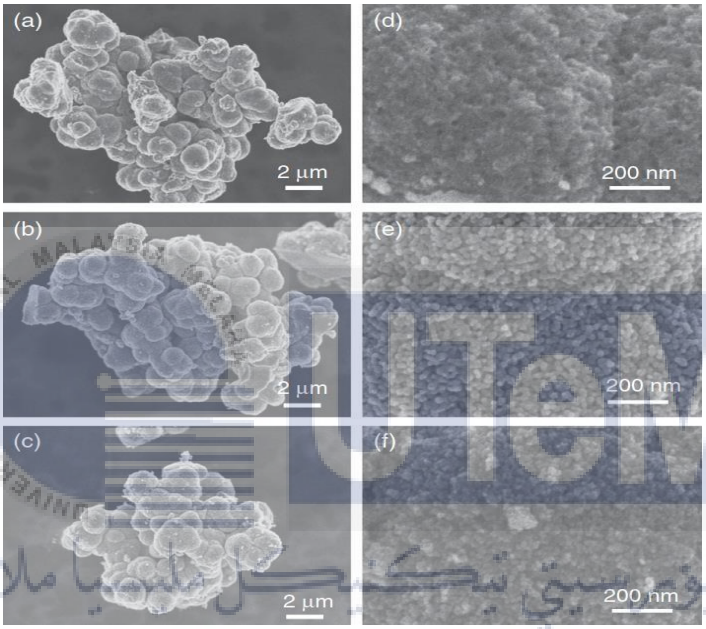

Figure 2.17: The FE-SEM images taken at low magnification of (a) as-synthesized, (b) annealed and (c) hydrothermal treated TiO2 powders; and at high magnification of (d) assynthesized, (e) annealed and (f) hydrothermal treated TiO2 powders

Winnicki et al. (2019) reported that the surface topography, thickness and density of the coatings are highly dependent on the phase powder content and the preheating temperature of the gas. Powders had differing sizes and mass density due to the development of agglomerates, which greatly affected the spraying method and the deposition quality. The maximum deposition quality attained for amorphous, anatasic and rutile powders using working gas heated to 600 °C was 25 percent, 17 percent and 3 percent, respectively. Coating deposited at the lowest gas temperature displayed the poorest consistency. Amorphous powders culminated in a satisfactory deposition of the powder. The thickness of the coating was up to 50 μm. However, coatings have been distinguished by delamination, microcracks and porosity (Fig.

2.18 a, b). Anatase (Fig. 2.18 c, d) and rutile (Fig. 2.18 e, f) formed very thin films on the aluminium substrate. It took the shape of submicron particles enclosed on the surface of the substrate. Coating roughness comes from sand-blasting layer or local accumulation of agglomerated powder particles. However, it was difficult to achieve a thicker coating separately on the amount of coating layers sprayed onto the substrate content.

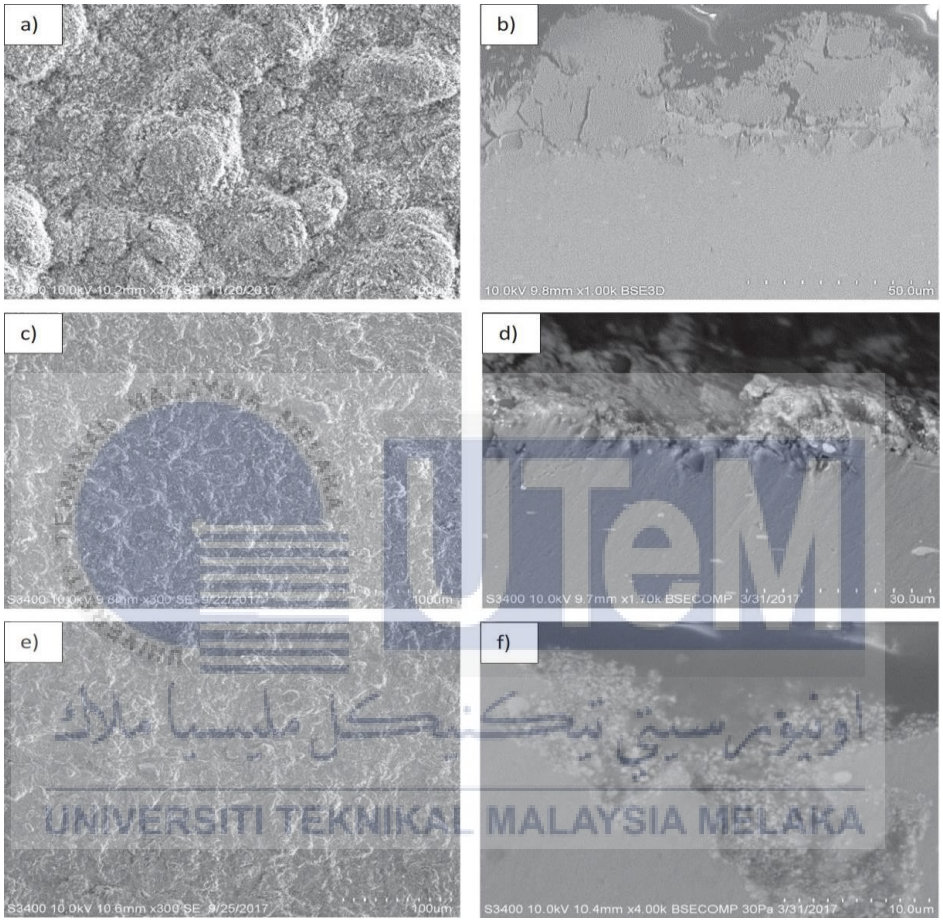

Figure 2.18: Micrographs (SEM) of coatings sprayed with the use of amorphous (a,b), anatase (c,d) and rutile (e,f) powders and air preheated to 200 °C, coatings surface (SE) (a,c,e) and cross section (BSE) (b,d,f).

CHAPTER 3

METHODOLOGY

This chapter outlines the proposed methodology for this research, which consists of the concepts of the sample preparations, the procedure, heat treatment and method to characterize the properties of TiO2.

3.1 Introduction

The methodology for this work was outlined in the flow chart available, as shown in Figure 3.1. This project involves three main part which are important to the development of TiO2. The three main parts are preparation of TiO2 sample, calcination of TiO2 and characterization of the TiO2 that undergoes calcination

3.2 Flowchart of Overall Proposed Research

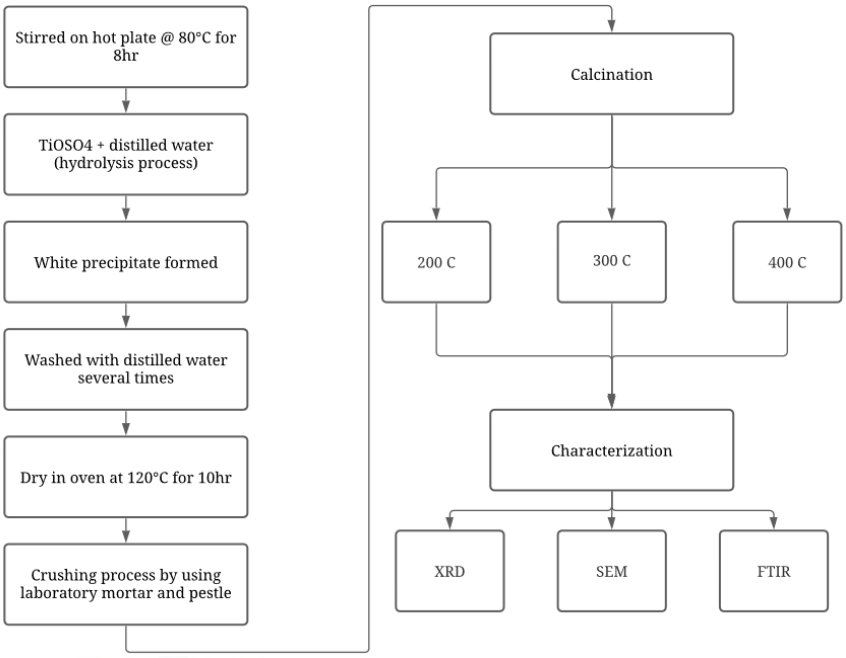

Figure 3.1: Flow Chart

3.3 Preparation of TiO2 samples

The TiO2 powder, which was synthesised in this work, was made by simple hydrolysis. Titanyl sulphate solution was prepared by combining the titanyl sulphate powder with the distilled water. Theoretically, the involve reaction of titanyl sulphate (TiOSO4) and water will be obtained TiO2 powder with the chemical equation.

$$TiOSO4 + H2O \rightarrow TiO2 + H2SO4 \qquad \text{Equation 1}$$

The first step in this methodology is filled a 100 gm of titanyl sulphate powder into a 1000 ml beaker. The weight of titanyl sulphate was determined by using the laboratory electronic balance. The ratio of TiOSO4 to distilled water was 1:9, therefore, 900 ml of distilled water was added to the beaker that already filled with the TiOSO4. After that, the beaker was transferred on the top of hot plate for the next step as shown in Figure 3.2.

Figure 3.2: Beaker filled with TiOSO4 powder was on a hot plate

The hydrolysis process started by stirring on hot plate at 80ºC for 8 hours. The 8-hour calculation begun right after the solution turns from transparent (Figure 3.3) to the white solution (Figure 3.4) like the early phase of this process. During the 8-hour countdown it is important to make sure that solution was always in 80 ºC. To prevent the solution from getting out of the range from the temperature that had been set, the solution was checked frequently with the thermometer for about 10-15 minutes time interval.

Figure 3.3: The solution turn into transparent

Figure 3.4: The solution turns back into white solution from transparent

Finished after 8-hour mark, the white precipitate was formed as shown in figure 3.5. The white precipitate formed were then washed with distilled water for several times up to 5 days for cleaning process.

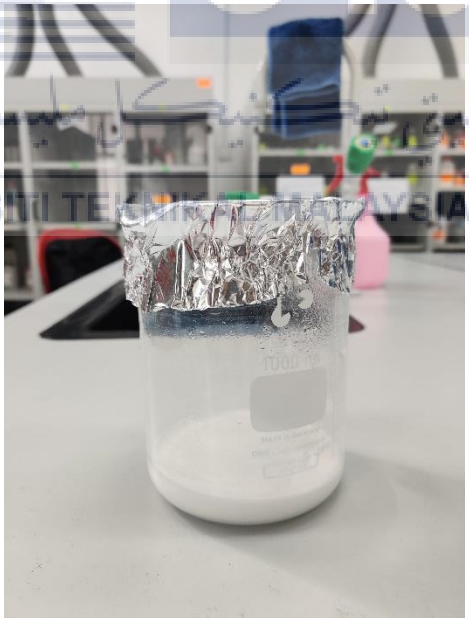

Figure 3.5: White precipitate formed

After 5 days of cleaning process, the white precipitate was place in the oven at 120ºC for 10 hours for drying process. The main purpose for this drying process is to get rid the

excessive water that still presence in the white precipitated. Other than that, it is to make sure that result for characterization after this will be more accurate without the interfering of any other factor besides the calcination temperature. Finally, the last step in this preparation of TiO2 sample is a crushing process by using laboratory mortar and pestle. Crushing process is a must because after the TiO2 undergoes drying process, the powder will be in a lumpy state, and to solve this issue, reducing the size of material by crushing process wil be applied. The TiO2 powder is divided into 4 samples which was labeled as (a) as-synthesize, (b) calcine at 200ºC, (c) calcined at 300ºC and (d) calcined at 400ºC.

3.4 Calcination

The heat treatment that will be used in this project is calcination. Calcination is a process of heating a material to a high temperature but below its melting or fusing point, resulting in moisture loss, reduction or oxidation, and dissociation into simpler compounds. The word was initially used to the process of removing carbon dioxide from limestone in order to produce lime (calcium oxide). Calcination is also used to recover metals from ores. The TiO2 powder samples were calcined at 200ºC, 300ºC, and 400ºC for 1 hour each. Figure 3.6 shows the calcination furnace.

Figure 3.6: calcination furnace

3.5 Characterization of TiO2 Powder

X-ray diffraction (XRD) patterns were produced for the characterisation using a Rigaku RINT 2500 with Cu-Ka radiation (=1.5406 A) throughout the 2 range of 20–80. The morphology of the resultant powders and the collected broken cross sections of the coated samples were investigated using a scanning electron microscope (SEM) (SEM: JSM-6390, JEOL). Fourier transform infrared spectroscopy (FTIR) investigations in the 400–4000 cm1 frequency range were performed to evaluate TiO2 bonding.

CHAPTER 4

RESULT AND DISCUSSION

This chapter will discuss the results obtained to determine and understand more about the effect of heat treatment on the morphology of TiO2 powders. In this chapter, the XRD analysis will be discussed based on my data collected during the lab work. Meanwhile, the SEM and FTIR analysis will be discussed based on various previous research data. In this XRD analysis, we can determine its phase and its crystallite size

4.1 X-Ray Diffraction (XRD) Analysis

Analysis of X-ray diffraction (XRD) is a method for determining the crystallographic structure of a material used in the fields of material science. XRD works by irradiating an incident X-ray material to measure then the intensity and dispersion angles of the X-ray, which leave it. In this XRD analysis, we can determine its phase and its particle size.

Figure 4.1 shows the XRD pattern of the synthesized TiO2 powder with different value of calcination temperature. In order to determine the phase of this TiO2 powder, The phases of the tested powders were identified by matching the observed XRD patterns to PDF Card No. 021-1272. For photocatalysis applications, a single-phase anatase structure is very desired. After the heat treatments, crystallinity improves, as shown by sharper and higher attenuation of diffraction peaks.

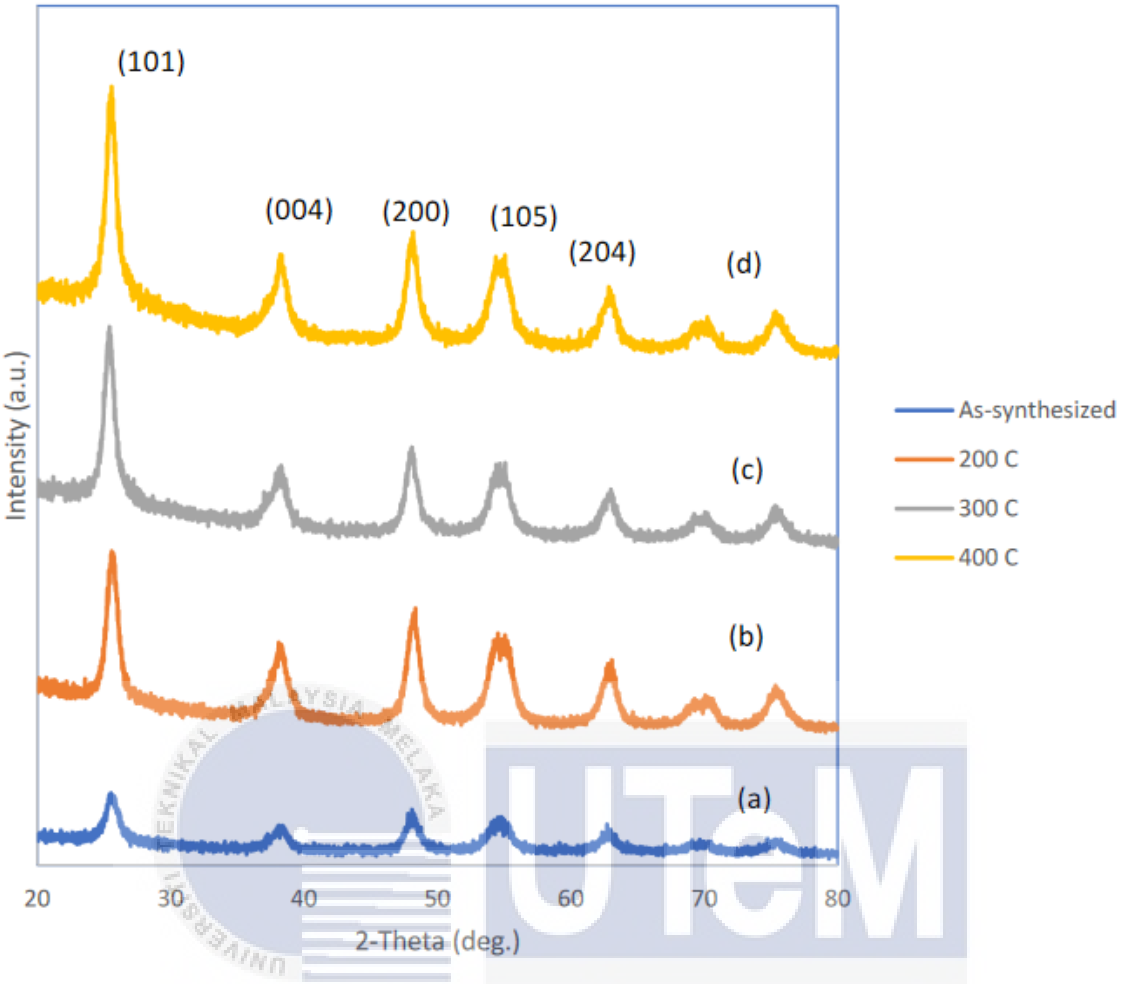

Figure 4.1: XRD pattern of different sample of TiO2 powder with different calcination temperature

The crystallite size was calculated by using the Scherrer equation, the full width at half maximum (FWHM) and the most intense peak data of their XRD patterns was determined from the raw data that had been obtained. Table 4.1 shows that there is increasing in the crystallite size when the calcination temperature is increase. The broad diffraction peaks showed that all the tested powders were in anatase phase with nanometer sized. Low-temperature calcination improved the crystallinity and crystallite size of the as-synthesized TiO2 powders.

Table 4.1: Crystallite size of TiO2 powder with different calcination temperature

Calcination temperature (°C)	Crystallite size (nm)
As synthesized	3.69
200	5.09
300	5.24
400	6.61

However, from the findings we can see that even though with the powders calcined at 200°C, 300°C, and 400°C, only a small increase in crystallinity and crystallite sizes was found. This shows that calcination does improve the crystallinity and crystallite size of TiO2 powder. The improvement of crystallinity can also be determined by calculated the crystallinity percent on each of the TiO2 samples. The crystallinity percent as presented in the table 4.2

Table 4.2: Crystallinity percent of TiO2 with different calcination temperature

Calcination temperature (°C)	Crystallinity (%)
As synthesized	90.6578
200	94.30879
300	96.63732
400	96.77902

4.2 Review on SEM Morphology

Figures 4.3 and 4.4 illustrate the particle morphologies of TiO2 powders following synthesis and calcination at 200°C, 300°C, and 400°C, respectively. This is the reviewed result from the work done by Toibah et al., (2016), despite the powders being calcined up to 400°C, there were no noticeable changes in particle size. But as seen in figure 4.4, calcination of powders enhanced particle density by lowering the number of holes. This SEM image indicates that this reviewed is consistent with the previous result in the XRD analysis that had been discuss earlier.

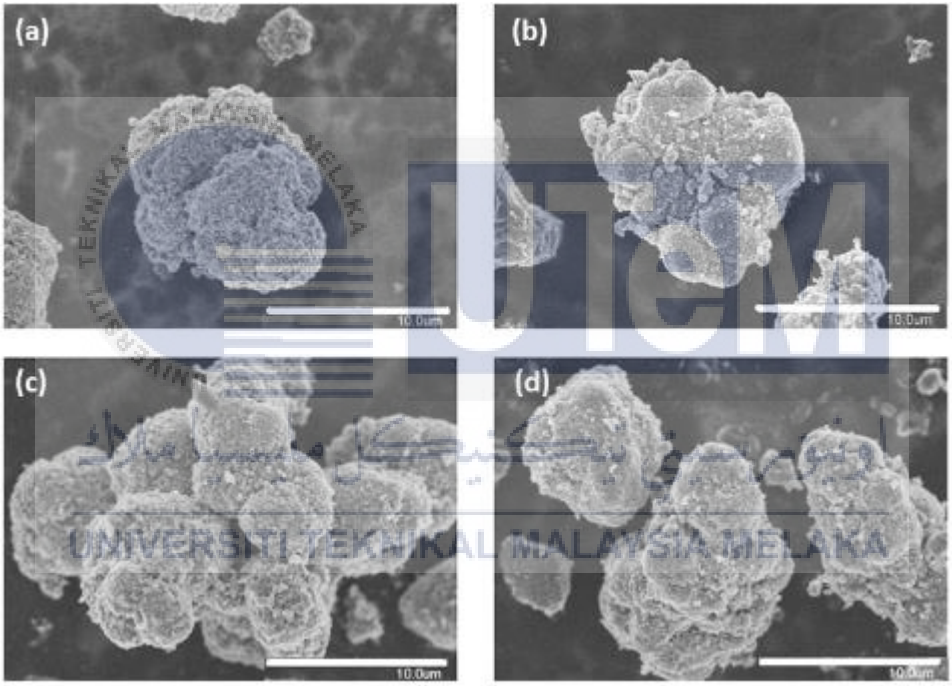

Figure 4.3: SEM micrographs of TiO2 powders calcined at different temperatures: (a) as-synthesized powder (TiO2-0), (b) TiO2 powder calcined at 200°C (TiO2-2), (c) TiO2 powder calcined at 300°C (TiO2-3) and (d) TiO2 powder calcined at 400°C (TiO2-4). (Toibah et al., 2016)

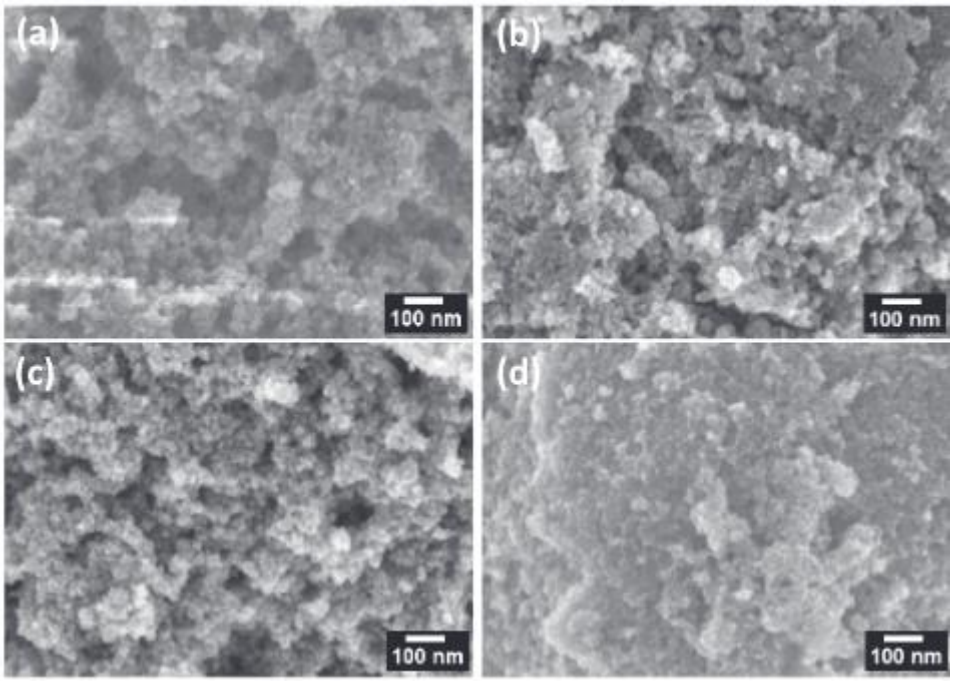

Figure 4.4: SEM images taken at high magni-cation of TiO2 powders calcined at different temperatures: (a) as-synthesized powder (TiO2-0), (b) TiO2 powder calcined at 200°C (TiO2-2), (c) TiO2 powder calcined at 300°C (TiO2-3) and (d) TiO2 powder calcined at 400°C (TiO2-4) (Toibah et al., 2016)

Araoyinbo et al. (2018) was analysed morphology on two sample of TiO2 with calcination temperature at 400°C and 700°C respectively by SEM images under 10 kx magnification. From the figure 4.5, at 400°C, titanium dioxide nanoparticles seem much more homogeneous on the surface, whereas increasing temperature to 700°C, results in a larger particle size and greater agglomeration as shown in figure 4.6. Here, we can justify that heat treatment has a serious influence on particle size, as seen by these data.

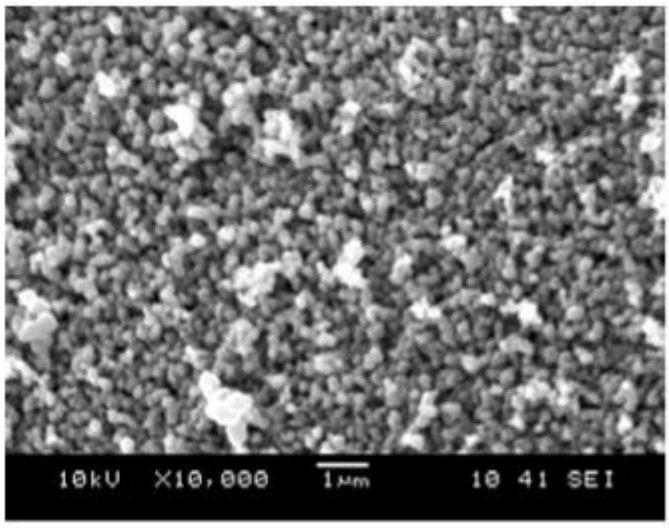

Figure 4.5: Titanium dioxide nanoparticles calcined at 400°C (Araoyinbo et al., 2018)

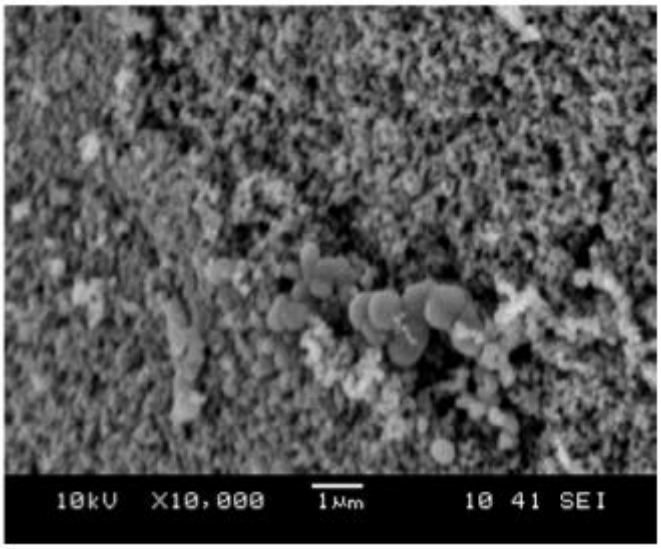

Figure 4.6: Titanium dioxide nanoparticles calcined at 700°C (Araoyinbo et al., 2018)

The greater the specific surface area, the smaller the catalyst. Calcination temperature is also crucial for eliminating organic compounds from the final products and finishing crystallisation. A very high calcination temperature will result in aggregation and phase change, which will impact the microstructures as well as the characteristics of titanium dioxide nanoparticles.

From both works, calcination at 400°C shows a similarity in terms of particles distribution. It also shows a denser microstructure compare at lower temperature. Other than that, both of this works also shows that it is corresponding with research by Salim et al. (2011). Salim et al. (2011) stated that TiO2 that undergoes heat treatment for 400° C and above will face difficulty in result in a lack of ability to build up the coating during impact during coating application process.

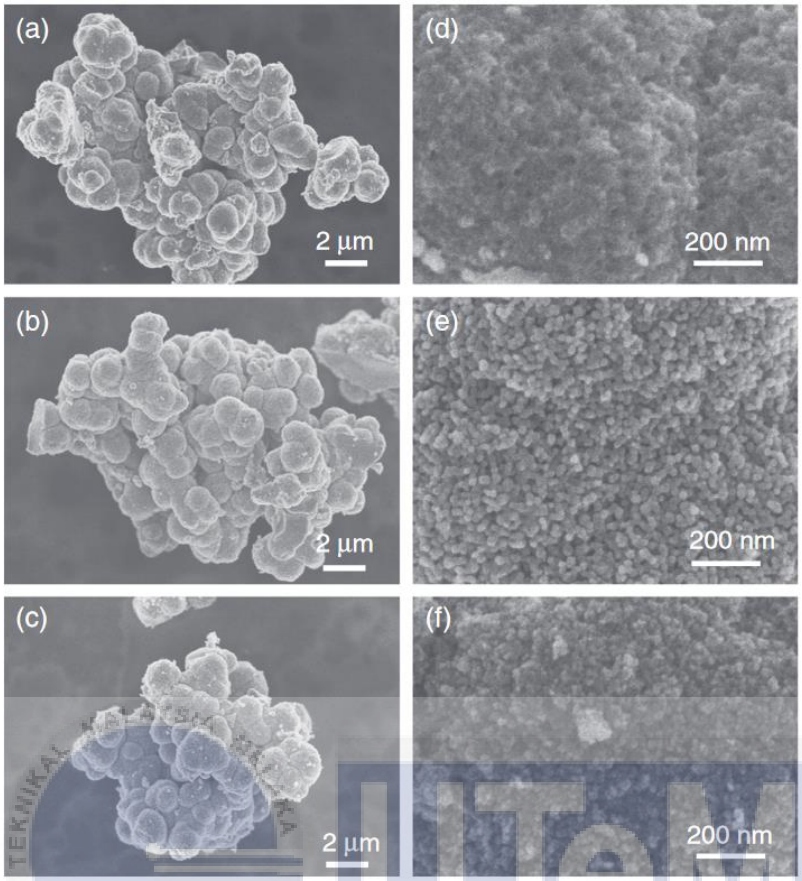

Figure 4.7: The FE-SEM images taken at low magnification of (a) as-synthesized, (b) annealed at 600°C and (c) hydrothermal treated TiO2 powders; and at high magnification of (d) as-synthesized, (e) annealed and (f) hydrothermal treated TiO2 powders (Salim et al., 2011)

From this reviewed analysis, when the powders were calcined from 200°C to 400°C, no significant results were discovered that contributed to the progressive improvement in crystallinity and density. However, it is probable that crystalline bridges between the primary particles got stronger as the calcination temperature was increased up to 400°C. The SEM picture of TiO2 powders shows a reduction in the average size of the pores, which play an essential role in particles attraction. This might be attributed to the greater degree of crystallinity and the development of strong agglomerated particles by a densification of particles during the heat treatment at higher calcination temperature. Due to that, the particles were tightly bound and it was difficult to shatter these hard agglomerated particles, which had a lower porosity.

4.3 Review on Fourier Transform Infrared Spectroscopy (FTIR) Analysis

FTIR analysis is a method of identifying organic, polymeric, and, in certain circumstances, inorganic materials. The FTIR analysis method scans test materials using infrared light to evaluate chemical characteristics. In this part the FTIR will be used to determine the scale presence of TiO2.

Horti et al. (2019) had reported FTIR spectra for 6 different samples of TiO2 which are as-synthesized (C0) as-synthesized (C0), calcined at 300 C (C3), calcined at 400 C (C4), calcined at 500 C (C5), calcined at 600 C (C6). A FTIR of TiO2 nanoparticle spectrum is shown in Figure 4.8. C0, C3, C4, C5 and C6 are represented by curves a–e, respectively.

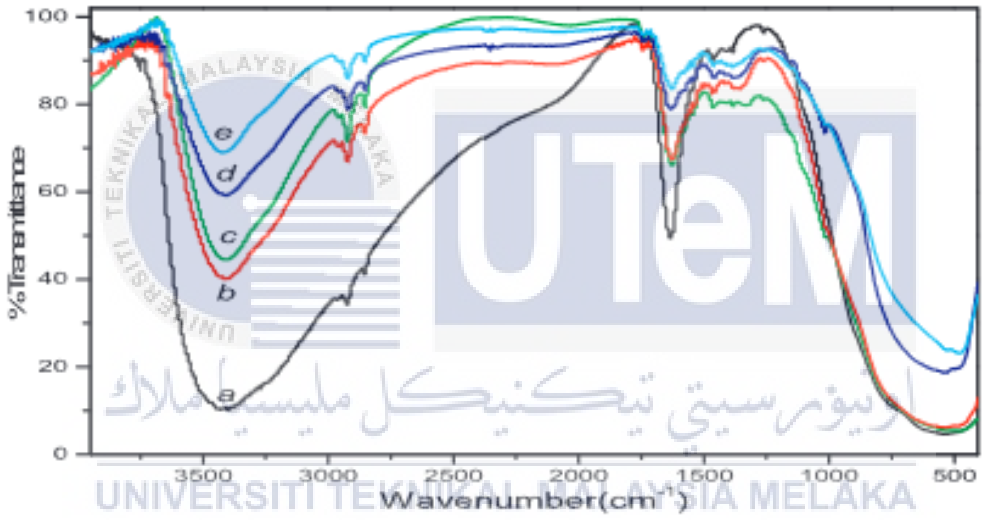

Figure 4.8: FTIR spectra of TiO2 nanoparticles, Curves a–e respectively, represent FTIR spectrum for samples C0, C3, C4, C5 and C6.

To verify the presence of TiO2 as a crystalline phase, the absorption band detected between 400 cm-1 and 800 cm-1 is linked with bending vibration bonds in the TiO2 lattice (O-Ti-O) At 1620 cm-1, a sharp peak has appeared, and it represents the typical bending vibration of an OH-group molecule. In the region of 3200 to 3800 cm-1, the broad absorption peak is due to the interaction between TiO2 and the hydroxyl group of the water molecules. From the figure, higher calcination temperature reduces the intensity of higher absorption bands, indicating that water molecules are removed from the sample and particles growth.

Sugapriya et al. (2013) had reported FTIR spectrum of annealing TiO2 nanoparticles. The TiO2 was annealed at 450ºC and 900ºC respectively. Figure 4.9 shows FTIR spectra of the annealed samples.

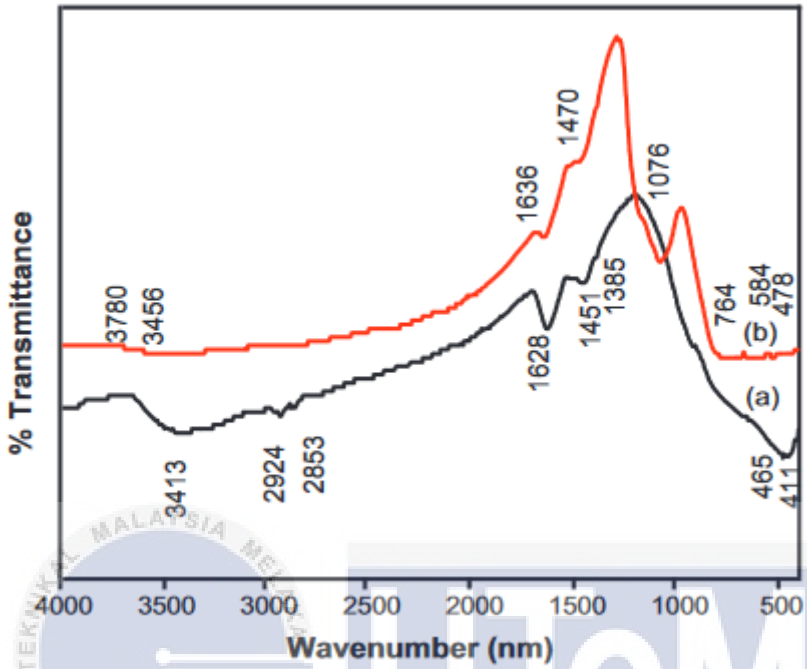

Figure 4.9: FT-IR spectrum of annealed TiO2 nanoparticles (a) 450 ◦ C and (b) 900 ◦ C (Sugapriya et al., 2013)

The spectra of TiO2 that has been annealed at 450 ºC is depicted in Fig. 4.9(a). OH groups in TiO2 nanoparticles have a stretching vibration mode that may be ascribed to the broad peak at 3413 cm-1, which is also assigned to the symmetric and antisymmetric OH modes of molecular water in TiO2 nanoparticles. At a wavelength of 1628 cm-1, the bending vibration associated with the molecular water bending band may be seen. The hydrolysis process results in the formation of TiO2 OH bonds. While the narrow bands at 2924 and 2853 cm-1 are attributed to organic residues arising from the sample because of the preparation method, the broad bands at 2924 and 2853 cm-1 are due to organic residues coming from the sample as a result of the preparation technique. In-plane skeletal vibrations of aromatic rings are responsible for the formation of the band at 1451 cm-1. The bending vibrations of Ti O and Ti O Ti framework bonds are attributed to the bands at 465 and 411 cm-1 in the low-energy area of the spectrum in the low-energy region of the spectrum.

When the annealing temperature is increased to 900 C (Fig. 4.9(b)), the intensity of the OH vibration bands and the Ti O bending vibration bands shifts to higher energy

attributed to the phase change from anatase to rutile. The annealing process causes the primary anatase band to move between 411 and 465 cm1, as well as the development of additional bands at 478 and about 764 cm1. The shift of the major adsorption at 465 cm1 and the increasing intensity of the band around 764 cm1 are usually ascribed to crystal phase transition from anatase to rutile with particle size variations.

From this previous work data, we can identify similarities in them. Both works show the same trend at a higher temperature, the less the intensity of higher absorption bands will occur. Furthermore, both results show the existence of TiO2 and OH resulting from the hydrolysis process at around 1620± cm-1 wavelength.

CHAPTER 5

CONCLUSION AND RECOMMENDATIONS

5.1 Conclusion

In this project, we can conclude that there are many effects of the heat treatment on the morphology of TiO2 that we can found. One of those things is, the calcined TiO2 does give a better crystallinity rather than the as-synthesized TiO2. For example, the as-synthesized crystallinity percent is just 90.6578% while the calcinated TiO2 does receive increasing of crystallinity around 3%-7% depend on the calcination temperature that had been set on the TiO2 sample. Other than that, higher calcination temperature increases the crystallite size but will reduced the porosity of TiO2 particle. A higher temperature of 400°C not only increases the development of grain and the crystallite size of TiO2 powders, but also decreases the porosity in powder agglomeration via particle densification. Next, the calcination temperature does affect the phase of the TiO2. At lower calcination, even though the crystallite size is increased and crystallinity percent, but usually the anatase phase still retain in it without experience transformation phase. It is another story with higher calcination temperature, where there is a presence of rutile phase alongside with anatase phase. This is the reason why this project chooses heat treatment with lower calcination temperature.``

5.2 Recommendations

There are several additional recommendations to improve this research further.

a) Preparation for the sample of TiO2 is the crucial part in this project and to follow prescribed procedures is compulsory

b) During the hydrolysis process it is important to ensure that the solution remains at the specified temperature level that had been decided, throughout the period hydrolysis occurs.

c) For the calcination process, it is advisable to use the same calcination furnace from start until end of the sample that been used for testing.

REFERENCES

Araoyinbo, A. O., Abdullah, M. M. A. B., Rahmat, A., Azmi, A. I., Vizureanu, P., & Wan Abd Rahim, W. M. F. (2018). Preparation of Heat Treated Titanium Dioxide (TiO2) Nanoparticles for Water Purification. *IOP Conference Series: Materials Science and Engineering*, *374*(1). https://doi.org/10.1088/1757899X/374/1/012084

Chen, Q., Liu, H., Xin, Y., & Cheng, X. (2013). TiO2 nanobelts - Effect of calcination temperature on optical, photoelectrochemical and photocatalytic properties. *Electrochimica Acta*, *111*, 284–291. https://doi.org/10.1016/j.electacta.2013.08.049

Gupta, S. M., & Tripathi, M. (2011). A review of TiO2 nanoparticles. *Chinese Science Bulletin*, *56*(16), 1639–1657. https://doi.org/10.1007/s11434-011-4476-1

He, F., Ma, F., Li, J., Li, T., & Li, G. (2014). Effect of calcination temperature on the structural properties and photocatalytic activities of solvothermal synthesized TiO2 hollow nanoparticles. *Ceramics International*, *40*(5), 6441–6446. https://doi.org/10.1016/j.ceramint.2013.11.094

Horti, N. C., Kamatagi, M. D., Patil, N. R., Nataraj, S. K., Sannaikar, M. S., & Inamdar, S. R. (2019). Synthesis and photoluminescence properties of titanium oxide (TiO2) nanoparticles: Effect of calcination temperature. *Optik*, *194*(April). https://doi.org/10.1016/j.ijleo.2019.163070

Jena, A., Vinu, R., Shivashankar, S. A., & Madras, G. (2010). Microwave assisted synthesis of nanostructured titanium dioxide with high photocatalytic activity. *Industrial and Engineering Chemistry Research*, *49*(20), 9636–9643. https://doi.org/10.1021/ie101226b

Lal, M., Sharma, P., & Ram, C. (2021). Calcination temperature effect on titanium oxide (TiO2) nanoparticles synthesis. *Optik*, *241*(March), 166934.

https://doi.org/10.1016/j.ijleo.2021.166934

Lee, H., Song, M. Y., Jurng, J., & Park, Y. K. (2011). The synthesis and coating process of TiO2 nanoparticles using CVD process. *Powder Technology*, *214*(1), 64–68. https://doi.org/10.1016/j.powtec.2011.07.036

Lee, K., Mazare, A., & Schmuki, P. (2014). One-dimensional titanium dioxide nanomaterials: Nanotubes. *Chemical Reviews*, *114*(19), 9385–9454. https://doi.org/10.1021/cr500061m

Liu, N., Chen, X., Zhang, J., & Schwank, J. W. (2014). A review on TiO2-based nanotubes synthesized via hydrothermal method: Formation mechanism, structure modification, and photocatalytic applications. *Catalysis Today*, *225*, 34–51. https://doi.org/10.1016/j.cattod.2013.10.090

Mahshid, S., Askari, M., & Ghamsari, M. S. (2007). Synthesis of TiO2 nanoparticles by hydrolysis and peptization of titanium isopropoxide solution. *Journal of Materials Processing Technology*, *189*(1–3), 296–300. https://doi.org/10.1016/j.jmatprotec.2007.01.040

Rahim, T. A., Takahashi, K., Yamada, M., & Fukumoto, M. (2016). Effect of powder calcination on the cold spray titanium dioxide coating. *Materials Transactions*, *57*(8), 1345–1350. https://doi.org/10.2320/matertrans.T-M2016817

Salim, N. T., Yamada, M., Nakano, H., Shima, K., Isago, H., & Fukumoto, M. (2011). The effect of post-treatments on the powder morphology of titanium dioxide (TiO2) powders synthesized for cold spray. *Surface and Coatings Technology*, *206*(2–3), 366–371. https://doi.org/10.1016/j.surfcoat.2011.07.030

Sugapriya, S., Sriram, R., & Lakshmi, S. (2013). Effect of annealing on TiO2 nanoparticles. *Optik*, *124*(21), 4971–4975. https://doi.org/10.1016/j.ijleo.2013.03.040

Wang, T. H., Navarrete-López, A. M., Li, S., Dixon, D. A., & Gole, J. L. (2010).

Hydrolysis of TiCl4: Initial steps in the production of TiO 2. *Journal of Physical Chemistry A*, *114*(28), 7561–7570. https://doi.org/10.1021/jp102020h

Winnicki, M., Baszczuk, A., Jasiorski, M., Borak, B., & Małachowska, A. (2019). Preliminary studies of TiO2 nanopowder deposition onto metallic substrate by low pressure cold spraying. *Surface and Coatings Technology*, *371*(July 2018), 194–202. https://doi.org/10.1016/j.surfcoat.2018.09.057

Xia, B., Huang, H., & Xie, Y. (1999). Heat treatment on TiO2 nanoparticles prepared by vapor-phase hydrolysis. *Materials Science and Engineering B*, *57*(2), 150–154. https://doi.org/10.1016/S0921-5107(98)00322-5

Zhou, Y., Zhang, L., & Tao, S. (2018). Porous TiO2 with large surface area is an efficient catalyst carrier for the recovery of wastewater containing an ultrahigh concentration of dye. *RSC Advances*, *8*(7), 3433–3442. https://doi.org/10.1039/c7ra11985b